Trans. Korean Soc. Noise Vib. Eng., 24(9) : 667~674, 2014
http://dx.doi.org/10.5050/KSNVE.2014.24.9.667

한국소음진동공학회논문집 제 24 권 제 9 호, pp. 667~674, 2014
ISSN 1598-2785(Print), ISSN 2287-5476(Online)

Transient Torsional Vibration Analysis of Ice-class Propulsion Shafting System Driven by Electric Motor

전기 모터 구동 대빙급 추진 시스템의 과도 비틀림 진동 분석

Ronald D. Barro* and Don Chool Lee†
로날드 디. 바로·이돈출

(Received February 12, 2014 ; Revised August 18, 2014 ; Accepted August 18, 2014)

Key Words : Electric Motor(전기 모터), Propeller-ice Interaction(프로펠러-대빙 상호작용), Resonance(공진), Transient Torsional Vibration(과도 비틀림 진동)

ABSTRACT

A ship's propulsion shafting system is subjected to varying magnitudes of intermittent loadings that pose great risks such as failure. Consequently, the dynamic characteristic of a propulsion shafting system must be designed to withstand the resonance that occurs during operation. This resonance results from hydrodynamic interaction between the propeller and fluid. For ice-class vessels, this interaction takes place between the propeller and ice. Producing load- and resonance-induced stresses, the propeller-ice interaction is the primary source of excitation, making it a major focus in the design requirements of propulsion shafting systems. This paper examines the transient torsional vibration response of the propulsion shafting system of an ice-class research vessel. The propulsion train is composed of an electric motor, flexible coupling, spherical gears, and a propeller configuration. In this paper, the theoretical analysis of transient torsional vibration and propeller-ice interaction loading is first discussed, followed by an explanation of the actual transient torsional vibration measurements. Measurement data for the analysis were compared with an applied estimation factor for the propulsion shafting design torque limit, and they were evaluated using an existing international standard. Addressing the transient torsional vibration of a propulsion shafting system with an electric motor, this paper also illustrates the influence of flexible coupling stiffness design on resulting resonance. Lastly, the paper concludes with a proposal to further study the existence of negative torque on a gear train and its overall effect on propulsion shafting systems.

요 약

선박의 추진축계는 외부 변동 부하에 의해서 축계 손상을 일으킬 수 있다. 이러한 추진축계의

† Corresponding Author ; Member, Marine Engineering Division, Mokpo National Maritime University
E-mail : ldcvib@mmu.ac.kr
Tel : +82-61-240-7219, Fax : +82-61-240-7201
* Member, Marine Engineering Division, Mokpo National Maritime University

‡ Recommended by Editor Hyung-Jo Jung

동역학적인 특성은 운전 중에 일어나는 공진을 견딜 수 있거나 또는 피하도록 설계 및 최적화 해야 한다. 이러한 공진은 대빙급 선박의 추진시스템의 설계에 요구되는 프로펠러에서 유체역학적인 상호작용에 기인한다. 추진축계는 프로펠러와 대빙 사이의 상호관계로 인한 과도부하와 시스템의 공진에 의해서 진지한 응력을 받게 된다. 이 논문은 대빙이 적용된 극지 연구 선박에서 추진축계의 과도비틀림 진동응답을 검토하고자 한다. 추진축계는 전기모터로 구동되는 원동기, 탄성커플링 기어 및 프로펠러로 구성되어 있다. 이론적인 해석은 프로펠러의 대빙 부하를 기진력으로 과도비틀림진동 해석을 수행하였다. 그리고 실선에서 비틀림 진동을 계측하고 공진점을 확인하고 이를 이용하여 추진축계 한계 설계 토크에 대한 적용된 평가 요소를 국제선급연합 규정과 비교하였다. 전기모터를 갖는 추진축계에서 공진을 초래하는 탄성커플링의 강성 선정의 영향을 검토하였다.

Nomenclature

[C] : Damping matrix
D : Diameter
D_{lim} : $1.81 \cdot H_{ice}$
d : Propeller hub diameter
H_{ice} : Ice thickness for machinery strength design
[K] : Stiffness matrix
[M] : Moment of inertia matrix
n : Rotational speed at bollard condition
$P_{0.7}$: Propeller pitch at 0.7R
Q : Torque
R : Radius of propeller
S_{qice} : Ice strength index for blade ice torque
{T} : Torque vector
$t_{0.7}$: Max. thickness at 0.7R
$\{T_e\}$: External excitation torque vector
$\{T_i\}$: Internal excitation torque vector
$\{\theta\}$: Angular amplitude vector

1. Introduction

The unpredictable responses of excitation loads during propeller–ice interaction in ice-class propulsion shafting systems are challenging[1]. Although classification societies have rules and provisions for the different designs of ice-class propulsion shafting systems, it is stated that not all aspects of design for cold climates are accounted for by Ice Rules[2]. The steady and transient state torsional vibration analysis will provide an overview of a propulsion system's overall dynamic characteristic.

However, each propulsion configuration will produce different vibratory responses, so continuous research is necessary to address this issue. An ice-class vessel propulsion shafting system with an electric motor, coupling, gear train, and azimuth propulsor configuration is analyzed in this paper. Table 1 lists the research vessel's propulsion shafting specifications. Figure 1 shows the propulsion shafting system configuration, and Fig. 2 shows the mass–elastic model of the system.

All propulsion components contribute to the overall dynamic characteristic, including the resonance in the transient state of the system.

Table 1 Propulsion shafting system specifications

Component	Description	
Thruster unit	Type Classification	US ARC 0.8 DNV ice-class polar 10
Motor	Type Power	Variable speed 5,000 kW
Gear	Type Material Reduction ratio	Cyclo palloid High alloy steel 17CrNiMo6 4.188:1
Propeller	Type Material Diameter No. of blade Maximum propeller Speed	Open, fixed pitch Stainless steel 4 m 4 186 rpm

Transient excitation of the electric motors takes place during start-ups, as oscillating torque develops owing to slippage between the rotor and stator fields[3]. On the other hand, the gear train excitation develops owing to dynamic loading or negative torque[4]. Including an optimally designed coupling in the system can create a change in the mode shapes and damping that dissipate the torsional stresses. However, in this type of marine propulsion system, the main source of resonance excitation is attributed to propeller–ice interaction.

As such, this study investigates the dominant stresses of transient torsional vibration of an ice-class motor-driven propulsion system vessel. Theoretical analysis of system loading and transient vibration using the Newmark method is reviewed along with actual vibration measurements conducted on the subject vessel. The flexible coupling stiffness value used in the analysis was simulated to study its effect on the dynamic characteristic of the system. A detailed summary of findings from the analysis follows thereafter.

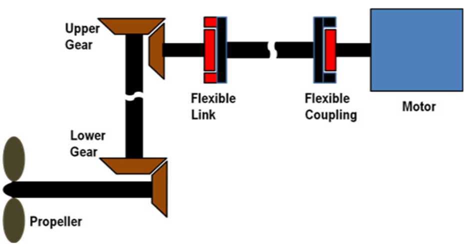

Fig. 1 Propulsion shafting configuration of subject vessel

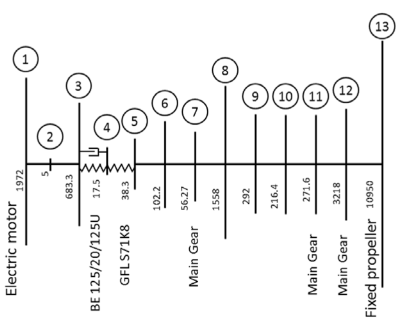

Fig. 2 Mass–elastic model of subject vessel

2. Measurement Data and System Excitation Loading Theoretical Analysis

2.1 Data Measurement and Torsional Vibration Analysis

To observe the dynamic characteristic of the propulsion shafting system, torsional vibration measurements were carried out on the subject vessel. Figure 3 shows the measuring points for the torsional vibration analysis. The measurements were carried out in accordance with KR Rules and Guidelines stating that the alternating torsional stress amplitude can be measured on a shaft in a relevant condition over a repetitive cycle. Figure 4 shows the laser vibrometer installation for data collection. The Engine and Vibration Monitoring System(EVAMOS) software designed by the Dynamics Laboratory of Mokpo National Maritime University was used to analyze the acquired data.

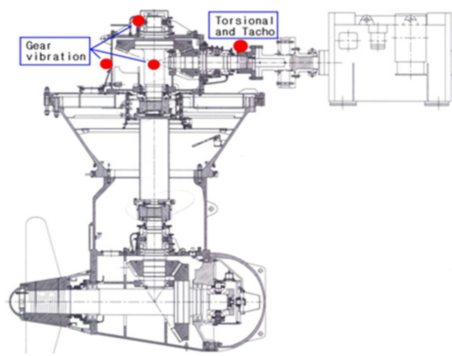

Fig. 3 Propulsion shafting system measuring points for torsional vibration

Fig. 4 Gap sensor positions for torsional vibration measurement

The results of torsional vibration analysis for the Geislinger Flexible Link coupling are shown in Figs. 5 and 6. Figures 6 and 7 are graphs of the calculated and measured 4^{th} order angular velocities of the coupling, respectively. The calculated and measured data show a significant disparity that may be due to the flexible coupling's dynamic stiffness and the motor rotor effective moment of inertia. According to Fig. 7, the torsional vibration resonance frequency occurs around 7.8 Hz and at an angular velocity amplitude of approximately 18.7 mrad/s.

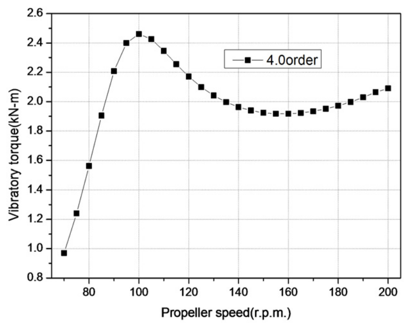

Fig. 5 Calculated vibratory torque of Geislinger flexible link in frequency domain

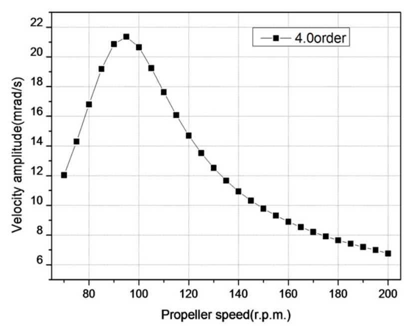

Fig. 6 Calculated angular velocity of Geislinger flexible link coupling motor side in frequency domain

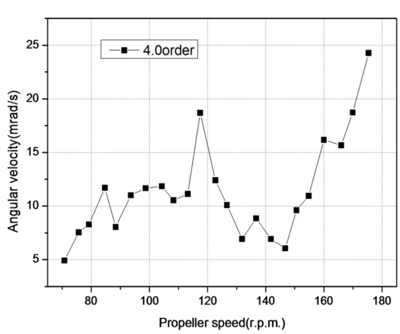

Fig. 7 Measured angular velocity of Geislinger flexible link coupling motor side

2.2 Transient Torsional Vibration Theoretical Calculation

The equation of motions can be solved by applying various step-by-step integration methods to obtain the dynamic behavior of the system under a specific loading, and the Newmark method is commonly used in dynamic response analysis(5). The Newmark method is applied since dynamic torsional stiffness shows a nonlinear aspect, depending on the vibratory torque transmitted(6). The equation of motion for a propulsion shafting system on torsional vibration can be expressed as follows:

$$[M]\{\ddot{\theta}\}+[C]\{\dot{\theta}\}+[K]\{\theta\}=\{T_i\}+\{T_e\} \tag{1}$$

The basic equation of the Newmark method is given in Eqs. 2 and 3.

$$\{\dot{\theta}\}_{t+\Delta t}=\{\dot{\theta}\}_t+\left[(1-\varepsilon)\{\ddot{\theta}\}_t+\varepsilon\{\ddot{\theta}\}_{t+\Delta t}\right]\Delta t \tag{2}$$

$$\begin{aligned}\{\theta\}_{t+\Delta t}=&\{\theta\}_t+\{\dot{\theta}\}_t\Delta t\\&+\left[(0.5-\eta)\{\ddot{\theta}\}_t+\eta\{\ddot{\theta}\}_{t+\Delta t}\right]\Delta t^2\end{aligned} \tag{3}$$

$$\begin{aligned}&[M]\{\ddot{\theta}\}_{t+\Delta t}+[C]\{\dot{\theta}\}_{t+\Delta t}\\&\quad+[K]\{\theta\}_{t+\Delta t}=\{T\}_{t+\Delta t}\end{aligned} \tag{4}$$

Substituting Eq. 1 with Eqs. 2 and 3, the equation of motion can be expressed as shown in Eqs. 5 to 7.

$$[\overline{K}]\{\theta\}_{t+\Delta t}=\{\overline{T}\}_{t+\Delta t} \tag{5}$$

$$\{\ddot{\theta}\}_{t+\Delta t}=a_0\left[\{\theta\}_{t+\Delta t}-\{\theta\}_t\right]-a_2\{\dot{\theta}\}_t-a_3\{\ddot{\theta}\}_t \tag{6}$$

$$\{\dot{\theta}\}_{t+\Delta t}=\{\dot{\theta}\}_t+a_6\{\ddot{\theta}\}_t+a_7\{\ddot{\theta}\}_{t+\Delta t} \tag{7}$$

$$[\overline{K}] = [K] + a_0[M] + a_1[C],$$
$$\{T\} = \{T_i\} + \{T_e\}$$
$$\{\overline{T}\}_{t+\Delta t} = \{T\}_{t+\Delta t} + [M]\left[a_0\{\theta\}_t + a_2\{\dot{\theta}\}_t + a_3\{\ddot{\theta}\}_t\right] + [C]\left[a_1\{\theta\}_t + a_4\{\dot{\theta}\}_t + a_5\{\ddot{\theta}\}_t\right] \quad (8)$$
$$a_0 = \frac{1}{\eta\Delta t^2},\ a_1 = \frac{2}{\eta\Delta t},\ a_2 = \frac{1}{\eta\Delta t},$$
$$a_3 = \frac{1}{2\eta} - 1,\ a_4 = \frac{\varepsilon}{\eta} - 1,\ a_5 = \frac{\Delta t}{2}\left(\frac{\varepsilon}{\eta} - 2\right),$$
$$a_6 = \Delta t(1-\varepsilon),$$
$$a_7 = \varepsilon\Delta t,\ \varepsilon \geq 0.5,\ \eta \geq 0.25(0.5+\varepsilon)^2$$

2.3 Propeller–ice Interaction Loading Theoretical Analysis

Under the rules of the Korean Registry of Shipping applied to open propellers(7), the maximum design ice torque on a propeller during propeller–ice interaction is given as follows:

$$Q_{max} = 105 \cdot \left[1 - \frac{d}{D}\right] \cdot S_{qice} \cdot \left[\frac{P_{0.7}}{D}\right]^{0.16} \cdot \left[\frac{t_{0.7}}{D}\right]^{0.6} \cdot (nD)^{0.17} \cdot D^3 \quad (9)$$

when $< D_{lim}$

$$Q_{max} = 202 \cdot \left[1 - \frac{d}{D}\right] \cdot S_{qice} \cdot [H_{ice}]^{1.1} \cdot \left[\frac{P_{0.7}}{D}\right]^{0.16} \cdot \left[\frac{t_{0.7}}{D}\right]^{0.6} \cdot [(nD)]^{0.17} \cdot D^{1.9} \quad (10)$$

when $D \geq D_{lim}$

In Table 2, the ice-class factors are listed by design ice thickness and ice strength index value for estimating propeller ice loads according to ship class type. Table 3 presents the milling sequences during propeller–ice interaction in three cases, taking into account the torque excitation parameters. The torque resulting from a single blade impact as a function of propeller rotation angle for the cases given in Table 2 is represented by Eqs. 11 and 12(8).

$$Q_\varphi = Q_{peak} \cdot \sin\left(\frac{180}{\alpha_1}\alpha\right),\ \text{when } \varphi = 0 \ldots \alpha_1 \quad (11)$$

$$Q_\varphi = 0,\ \text{when } \varphi = \alpha_1 \ldots 360 \quad (12)$$

where $Q_{peak} = C_q \cdot Q_{max}$

From Eqs. 11 and 12, the total ice torque of the subject vessel was calculated in accordance with the torque excitation parameters of Table 3. Ice-class classifications PC1, PC4, and PC7 were chosen for theoretical calculation.

In Figs. 8 to 10, the total theoretical ice torque values for Ice-Class PC1 for Cases 1–3 are shown to be around 2.562 MN-m, 3.416 MN-m, and 1.707 MN-m, respectively. In addition, the simulated calculation values for the PC4 classification ice torque for Cases 1–3 are 2.349 MN-m, 3.132 MN-m, and 1.565 MN-m, respectively. The ice torque value for Cases 1–3 for the PC7 classification are 1.396 MN-m, 1.862 MN-m, and 0.930 MN-m, respectively.

Table 2 Ice-class factors for estimating propeller–ice loads

Ice class	H_{ice}[m]	S_{ice}[-]	S_{qice}[-]
PC1	4.0	1.2	1.15
PC2	3.5	1.1	1.15
PC3	3.0	1.1	1.15
PC4	2.5	1.1	1.15
PC5	2.0	1.1	1.15
PC6	1.75	1.0	1.0
PC7	1.5	1.0	1.0

Table 3 Torque excitation parameters

Torque excitation	Propeller–ice interaction	C_q	α_1
Case 1	Single ice block	0.75	90
Case 2	Single ice block	1.0	135
Case 3	Two ice blocks (phase shift 45°)	0.5	45

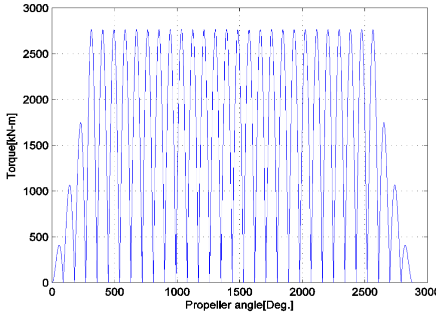

Fig. 8 Calculated total ice torque for Polar Class 1 – Case 1 excitation parameters

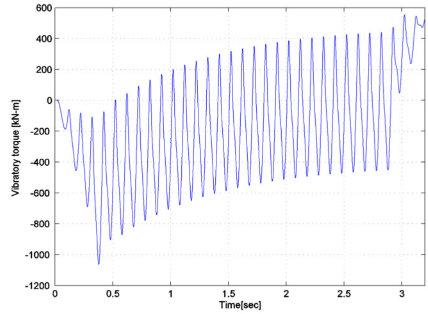

Fig. 11 Calculated transient vibratory torque response of electric motor

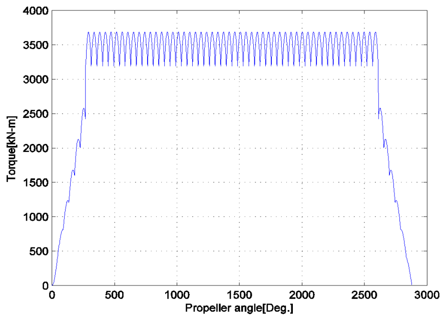

Fig. 9 Calculated total ice torque for Polar Class 1 – Case 2 excitation parameters

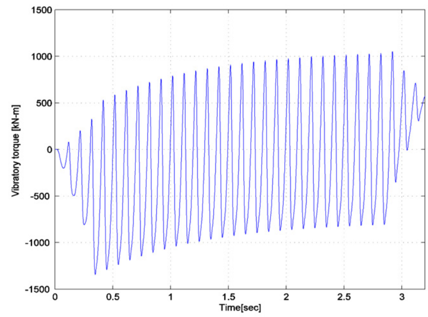

Fig. 12 Simulated transient vibratory torque response of electric motor with modified coupling stiffness

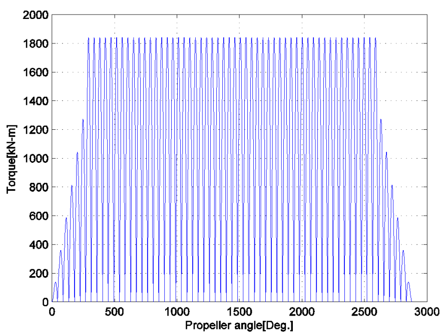

Fig. 10 Calculated total ice torque for Polar Class 1 – Case 3 excitation parameters

3. Vibratory Torque and Transient Torsional Vibration Analysis through Simulation

For transient torsional vibration analysis, four (4) mass members of the propulsion shafting system were observed for vibratory torque response. The electrical motor, flexible coupling, upper reduction gear, and lower reduction gear transient dynamic phenomena were analyzed through simulation. Measured torsional vibration data were utilized for simulating the transient vibratory torque due to torque from the ice impact acting on the propulsion shafting component. In addition, the flexible coupling was increased from 1.29 MN-m/s to 5.0 MN-m/s to observe its effect on the transient response of the system.

Figure 11 graphs the transient vibratory torque of the electric motor. The vibratory torque, considering Case 1 torque excitation parameters, is about 1.0 MN-m/s, while for the simulated response on lower flexible coupling stiffness(Fig. 12), the transient vibratory torque increased by about 30 % to 1.385 MN-m/s.

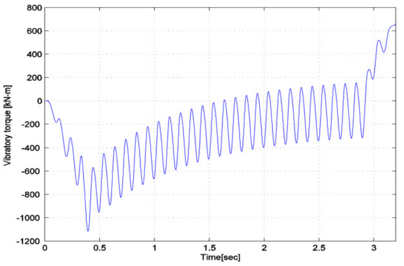

Fig. 13 Calculated transient vibratory torque response of flexible coupling

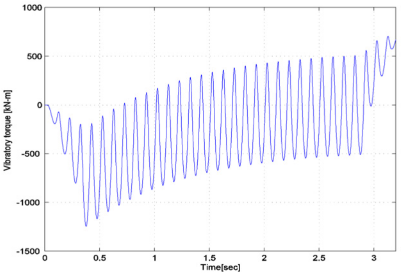

Fig. 14 Simulated transient vibratory torque response of flexible coupling with modified coupling stiffness

The calculated flexible coupling and modified transient vibratory torque responses are illustrated in Figs. 13 and 14. The calculated vibratory torque values are shown to be about 0.875 MN-m/s and 1.060 MN-m/s for simulated and modified flexible coupling stiffness, respectively. Figures 15 and 16 show the dynamic response on the upper reduction gear. The simulated transient vibratory torque was calculated to be approximately 1.5 MN-m/s. However, altering(lowered) of the coupling stiffness resulted in an increase in the vibratory torque value to 2.575 MN-m/s, which is approximately 40 % higher than the value with designed coupling stiffness.

Figures 17 and 18 indicate that the calculated and simulated vibratory torque responses of the lower reduction gear had the highest calculated value. The transient vibratory torque was around 2.15 MN-m/s. However, when the flexible coupling stiffness was modified, the vibratory torque value increased by only 5 % to 2.24 MN-m/s.

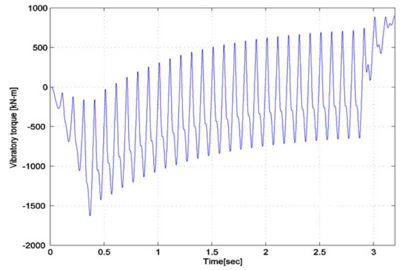

Fig. 15 Calculated transient vibratory torque response of upper reduction gear

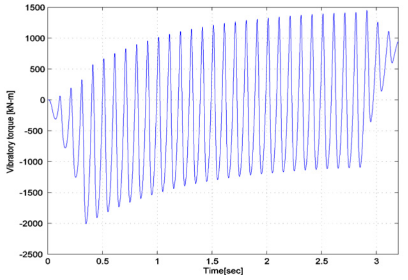

Fig. 16 Simulated transient vibratory torque response of upper reduction gear with modified coupling stiffness

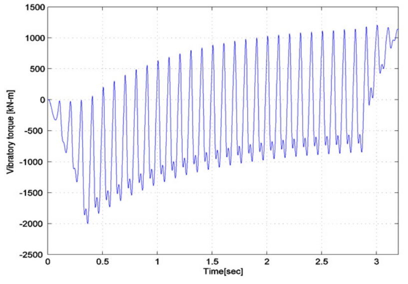

Fig. 17 Calculated transient vibratory torque response of lower reduction gear

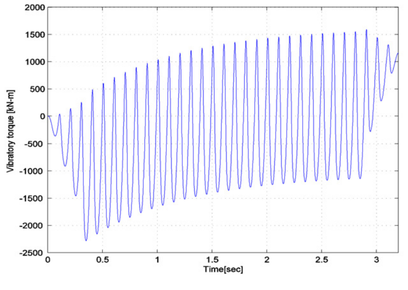

Fig. 18 Simulated transient vibratory torque response of lower reduction gear with modified coupling stiffness

3. Conclusion

This study investigated the transient torsional vibration response of an ice-class vessel through simulation using actual torsional vibration data and a modified flexible coupling stiffness factor. The subject vessel was installed with an electric motor as a prime mover and an azimuth propulsion configuration. The calculated vibratory torque of the propulsion shafting system components was compared with the design ice torque on the propeller. The following conclusions were made:

(1) Flexible coupling stiffness design influences the vibratory torque response of the propulsion shafting system.

(2) Dominant transient torsional stresses occurred on the lower reduction gear. Simulated theoretical calculation and modified flexible coupling stiffness calculation of its vibratory torque response both confirmed this phenomenon. Comparing these values with the propeller design ice impact torque limit, and considering the ship's ice classification, the range limit is close to the calculated transient vibratory torque.

(3) The high vibratory torque occurring on the reduction gear confirms the occurrence of negative torque during the propeller–ice interaction. This dynamic loading can be addressed through optimizing the gear train design and material specification. Further study on this propulsion shafting component resonance characteristic is recommended.

References

(1) Barro, R. D. and Lee, D. C., 2011, Excitation Response Estimation of Polar Class Vessel Propulsion Shafting System, Transactions of the Korean Society for Noise and Vibration Engineering, Vol. 21, No. 12, pp. 1166~1176.

(2) Gilmour, T. H., 2008, Arctic Shipping and Class, U.S. Maritime Administration Arctic Shipping Conference.

(3) Szolc, T. and Jankowski, L., 2008, Active Control of Transient Torsional Vibrations Due to Run-up of a Rotor Machine Driven by the Electric Motor, XXIII Symposium – Vibrations in Physical System.

(4) Szenasi, F. R. and Von Nimitz, W. W., 1978, Transient Analyses of Synchronous Motor Trains, Proceedings of the Seventh Turbomachinery Symposium.

(5) Chang, S. Y., 2004, Studies of Newmark Method for Solving Nonlinear Systems: (I) Basic Analysis, Journal of the Chinese Institute of Engineers, Vol. 27, No. 5, pp. 651~662.

(6) Lee, D. C. and Yu, J. D., 2003, Transient and Unstable Torsional Vibrations on a 4-stroke Marine Diesel Engine, ICES2003-578.

(7) Korean Registry of Shipping, 2012, Guidance Relating to the Rules for the Classification of Steel Ships.

(8) Batrak, Y., Torsional Vibration Calculation Issues with Propulsion Systems, ShaftDesigner – The Shaft Calculation Software.

Donchool Lee received his Dr. Eng. from Mechanical Engineering department at Korea Maritime University in 1995. He worked at Hyundai Heavy Industries from 1983 to 1999. He is now a professor of Mokpo National Maritime University.